Applied Physics Letters

Passivating the interface between halide perovskite and SnO_2 by capsaicin to accelerate charge transfer and retard recombination

Cite as: Appl. Phys. Lett. **120**, 103503 (2022); https://doi.org/10.1063/5.0082785
Submitted: 18 December 2021 • Accepted: 01 March 2022 • Published Online: 10 March 2022

Siyuan Lin, Pufeihong Xia, Shuyue Wu, et al.

Applied Physics Letters ARTICLE scitation.org/journal/apl

Passivating the interface between halide perovskite and SnO_2 by capsaicin to accelerate charge transfer and retard recombination

Cite as: Appl. Phys. Lett. **120**, 103503 (2022); doi: 10.1063/5.0082785
Submitted: 18 December 2021 · Accepted: 1 March 2022 ·
Published Online: 10 March 2022

Siyuan Lin,[1] Pufeihong Xia,[1] Shuyue Wu,[1] Wenhao Zhang,[2] Yue Hu,[2] Biao Liu,[1] Deming Kong,[1] Han Huang,[1] Yongli Gao,[3] and Conghua Zhou[1,a)]

AFFILIATIONS

[1]Hunan Key Laboratory of Super-Microstructure and Ultrafast Process in Advanced Materials, School of Physics and Electronics, Central South University, Changsha, Hunan 410083, People's Republic of China
[2]Michael Grätzel Center for Mesoscopic Solar Cells, Wuhan National Laboratory for Optoelectronics, Huazhong University of Science and Technology, Wuhan 430074, Hubei, People's Republic of China
[3]Department of Physics and Astronomy, University of Rochester, Rochester, New York 14627, USA

[a)]Author to whom correspondence should be addressed: chzhou@csu.edu.cn

ABSTRACT

Capsaicin is used to modify SnO_2 quantum dots and then used as an electron-transfer material for perovskite solar cells. After capsaicin modification, the power conversion efficiency of the devices increases from 19.90 (± 0.47)% to 21.87 (± 0.28)% with a champion device of 22.24% (AM 1.5G, 100 mW/cm^2). Transient photovoltage and photocurrent decay show that, after the capsaicin doping, the lifetime increases from 21.55 (± 1.54) to 27.63 (± 1.45) μs, while the charge extraction time reduces from 1.90 (± 0.09) to 1.67 (± 0.06) μs. Time-resolved photoluminescence and impedance spectrum studies show similar results. The accelerated charge transfer and retarded recombination are due to defect passivation. Space charge limited current study shows that, after modification, the trap density of devices is reduced from 2.24×10^{15} to 1.28×10^{15} cm^{-3}. X-ray photoelectron spectroscopy and theoretical calculation indicate that the reduced trap density is due to the chemical interaction between carbonyl group (from capsaicin) and Sn atom, and that between carbonyl group and Pb atom.

Perovskite solar cells (PSCs) have attracted broad attention due to the rapid growth of photo-to-electric power conversion efficiency (PCE), which has raised from 3.81% in 2009 to the recently recorded 25.5%.[1–5] Such performance is close to the crystalline silicon solar cells, though below the Schottky limit.[6,7] To reduce the efficiency gap, light harvest[8] and charge carrier transportation and recombination should be optimized.[9] Thus, wide adsorption active materials,[10] efficient charge transporting-materials,[11] tandem structure,[12] and interfacial and bulky modification strategies have been thoroughly studied.[13]

TiO_2 is widely used as electron-transport material (ETM) in PSCs with a n-i-p structure.[14,15] However, it usually requires high temperature (~450 °C) calcination and is highly UV-sensitive, which hinders practical applications.[16,17] Recently, low-temperature, solution basing SnO_2 arises as a promising alternative ETM due to the merits of high conductivity, inert photo-catalysis effect, and suitable band alignment.[18–20] In 2015, Yan and coworkers introduced low-temperature solution-processed SnO_2 into planar structured PSCs, obtaining PCE of 17.2%.[21] In 2016, You and coworkers developed planar PSCs using commercial colloidal SnO_2 nanoparticle as ETM and upgraded the PCE to over 20%.[20] In 2018, Fang and coworkers used SnO_2 quantum dots (SnO_2 QDs) as ETM in planar PSCs; they achieved PCE of 20.32%.[22] Later, Bawendi *et al.* developed a kind of chemical bath deposition method for SnO_2 and further promoted the PCE up to 25.2%.[4] Despite the successes, defects still remain at the interface between perovskite (PVSK) and SnO_2, which adds to non-radiative recombination and affects the fill-factor (FF) and open-circuit-voltage (V_{OC}) of devices.[23,24] As such, passivation is needed. For example, Fang and coworkers modified SnO_2 surface by an ultra-thin layer of fullerene and obtained PCE of 19.12% in 2016.[25] Liu and coworkers prepared an ethylene diamine tetraacetic acid-complexed SnO_2 layer to improve the energy band matching between SnO_2 and PVSK, which elevated V_{oc} and promoted PCE from 18.93% to 21.6%.[26] Wang *et al.* introduced RbF to SnO_2 colloid and helped to increase PCE to 23.38%.[27] Recently, Zhang and coworkers added

$CoCl_2 \cdot 6H_2O$ to SnO_2 films that improved energy level alignment and upgraded the PCE to 23.82%.[28] From these studies, one can see that passivation on PVSK/SnO_2 interface is an effective strategy to elevate device performance of PSCs.

Capsaicin (MW = 305.4) was previously introduced to the PSCs film by Bao and coworkers, which helped to obtain PCE of 21.88% in $MAPbI_3$ basing PSCs.[29] Coordination behavior was revealed between the carbonyl group (–C=O) from capsaicin molecule and Pb atom from PVSK, which led to defect passivation. Moreover, previous study showed that the amine group ($–NH_2$) could coordinate with Pb atom as well.[30] Coordination behavior also takes place when carbonyl group attaches to the surface of oxides, as observed in the study of dye-sensitized solar cells.[31,32] If such molecule could be added into the PVSK/SnO_2 interface, it could coordinate with both SnO_2 and PVSK, which is beneficial for defect passivation. As a result, here in this article, capsaicin is mixed with SnO_2 QDs and then used to prepare the ETM of PSCs. As will be shown later, passivation is realized at the PVSK/SnO_2 interface. Consequently, charge transfer is accelerated and charge recombination is retarded, which then helps to obtain PCE of 21.87 (± 0.28)% (champion at 22.24%) under AM1.5G illumination (100 mW/cm^2), with improved storage-stability in addition.

Fabrication processes of the device, materials, and reagent, along with the characterization methods are included in the supplementary material. To explore the passivation of capsaicin on device performance, capsaicin was mixed with SnO_2 QDs with varied concentration ratio (in mass). Four kinds of concentration ratios were chosen between capsaicin and SnO_2 or 0, 1%, 2%, and 4%. PSCs with structure of "FTO/SnO_2 @ capsaicin/PVSK/Spiro-OMeTAD/Ag" were fabricated, using $FA_xMA_{1-x}Pb(I_yBr_{1-y})_3$ as the active layer and capsaicin-containing SnO_2 QDs as the ETM. Device structure was shown in Fig. S1. Transmission electron microscope (TEM) image of SnO_2 QDs (size of ~3 nm) and schematic of capsaicin molecule are shown in the inset of Fig. 1(a).

Typical current-density vs voltage (JV) curves are shown in Fig. 1(a). One can see that the incorporation of capsaicin improves the device performance. Briefly, it increases the PCE from 20.34% to 22.24%. To show more details about the effect brought by capsaicin, statistics are performed on the performance parameters, with respect to the concentration ratio. As shown in Figs. 1(b) and 1(c) and 1(e) and 1(f), all of the three parameters are improved. For example, V_{oc} increases from 1.06 (± 0.02) to 1.08 (± 0.01) V, J_{sc} raises from 24.76 (± 0.21) to 25.18 (± 0.13) mA/cm^2, FF increases from 76.32 (± 2.14)% to 80.47 (± 0.78)%, incorrespondence, the PCE upgrades from 19.90 (± 0.43)% to 21.87 (± 0.28)%, ratio 2% comes out with the optimized performance, reaching 22.24% [as shown in Fig. 1(a)], for devices with doping ratio of 2%, 1.08 V of V_{oc}, 25.23 mA/cm^2 of J_{sc}, 81.27% of FF, and 22.24% of PCE are obtained from reverse scan, compared to 1.05 V (V_{oc}), 24.86 mA/cm^2 (J_{sc}), 78.32% (FF), and 20.34% (PCE) for the control device. External quantum efficiency (EQE) is tested [Fig. 1(d)], integrated J_{sc} is 24.67 mA/cm^2 for the device in the case of 2%, and 23.88 mA/cm^2 for the control device, corresponding to 97.78% and 95.79% of the J_{sc} recorded from JV curves test (reverse scans), respectively. It is interesting that capsaicin doping could affect the matching degree between the integrated and JV-tested J_{sc}. Such behavior might relate to the defect passivation. Since the EQE test is a kind of week signal test, defect-related trapping/de-trapping behavior is expected during the test; higher defect density would lead to lower EQE due to the trapping/de-trapping processes. Due to the

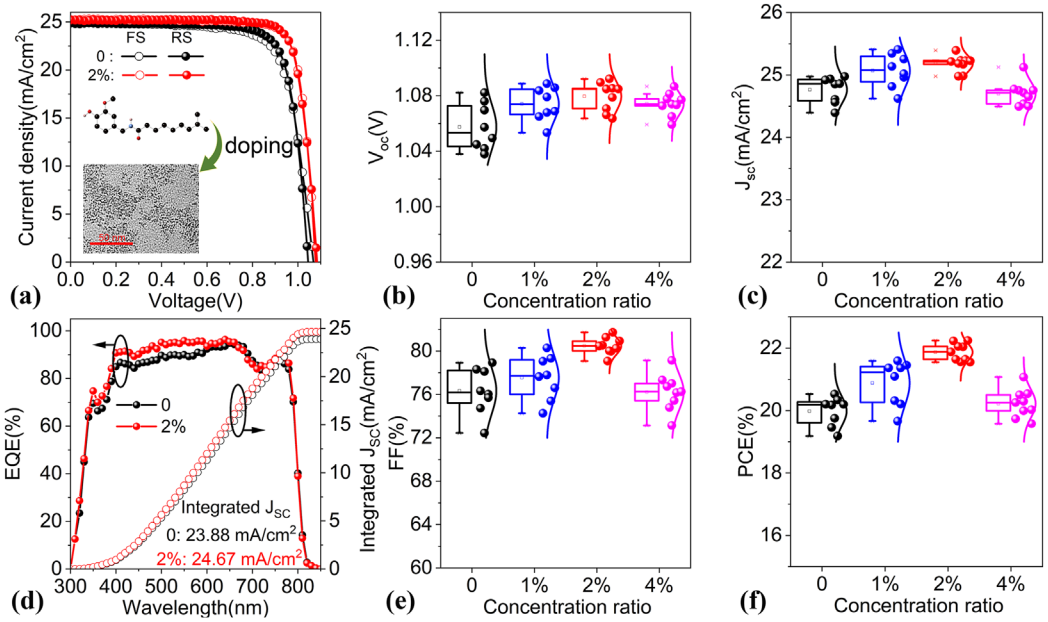

FIG. 1. (a) Typical current density–voltage (JV) curves of control device and device comprising 2% capsaicin in SnO_2 ETM (JV curves were recorded under simulated illumination of AM 1.5G, with the intensity of 100 mW/cm^2; "FS/RS" represent forward/reverse scans, respectively); the inset is the schematic of capsaicin molecule and TEM image of synthesized SnO_2 QDs. (d) The external quantum efficiency (EQE) spectra and integrated photocurrent. The statistical distribution of performance parameters for (b) V_{oc}, (c) J_{sc}, (e) FF, and (f) PCE.

passivation behavior brought by capsaicin molecules, lower defect density is anticipated (as seen in the SCLC test, Fig. 2); the matching degree then increases.[33]

Charge recombination and transfer kinetics are studied by transient photovoltage/photocurrent (TPV/TPC) curves. TPV decay curves under open-circuit conditions are used to characterize the recombination process happens in the solar cells; typical curves are shown in Fig. S2(a). Lifetime (τ) is fitted from the TPV curves, and the results are collected in Fig. 2(a). It is 21.55 ($\pm$ 1.54), 25.52 ($\pm$ 0.94), 27.63 ($\pm$ 1.45), and 24.78 ($\pm$ 0.61) μs for the concentration ratio of 0, 1%, 2%, and 4%, respectively. Obviously, lifetime of photo-generated charge carriers is prolonged after capsaicin doping, while 2% brings the longest one. TPC curves are used to characterize the charge transfer process; typical curves are depicted in Fig. S2(b). Charge transition time (t_d) is extracted from the TPC curves, and the results are shown in Fig. 2(b). It is 1.90 ($\pm$ 0.09), 1.82 ($\pm$ 0.07), 1.67 ($\pm$ 0.06), and 1.86 ($\pm$ 0.08) μs for the concentration ratio of 0, 1%, 2%, and 4%, respectively. As such, moderate capsaicin doping is beneficial for the charge extraction process. 2% produces the fastest charge extraction. Similar phenomenon is observed in impedance spectra (IS) studies [typical Nyquist plots are seen in Figs. S2(c) and S2(d)]. It could be found that capsaicin could affect both of the charge transfer resistance and recombination resistance (R_{ct} and R_{re}, respectively). As for R_{ct} [shown in Fig. 2(c)], it is 4.24 ($\pm$ 0.62), 3.45 ($\pm$ 0.42), 2.22 ($\pm$ 0.67), 3.42 ($\pm$ 0.47) $\times$ 10^4 Ω, and for R_{re} [shown in Fig. 2(d)], it is 0.85 ($\pm$ 0.16), 1.99 ($\pm$ 0.64), 2.32 ($\pm$ 0.54), and 1.56 ($\pm$ 0.39) $\times$ 10^7 Ω for the doping ratio of 0, 1%, 2%, and 4%, respectively. Obviously, capsaicin modification reduces the R_{ct} while increases the R_{re}. Again, 2% produces the smallest R_{ct}, but highest R_{re}. The behavior coincides well with TPC/TPV studies. Comparison between Figs. 2(a) and 2(b) could find that longer lifetime is helpful to obtain relatively higher V_{oc}, while faster charge extraction is favorable to obtain higher J_{sc}. This relation is quite similar to those observed before,[34–37] showing close relevance between these parameters. What is more, time-resolved photoluminescence (TRPL) spectra were also performed on PVSK that growing on ETM. Typical TRPL curves are shown in Fig. 2(e), and time constants are fitted from the curves and collected in Table S1 using the method described in the literature.[38] The average extract time is 14.20, 3.13, 2.44, and 14.7 ns for the doping ratio of 0, 1%, 2%, and 4% [shown in Fig. 2(f)], respectively. As will be seen later, crystallinity of PVSK films is improved when they grow on capsaicin doped SnO_2 QDs. Therefore, the reduced time constant is mainly due to the improved charge extraction processes. As a result, 2% produces the fastest charge extraction, which also coincides well with TPC and IS studies. Combination between these studies helps to see that capsaicin modification accelerates interfacial charge transfer while retards charge recombination processes.

The improved device performance and favored charge transfer (retarded recombination) processes are due to the passivation behavior brought by capsaicin molecules. Space charge limited current (SCLC) study is used to examine the trap density characteristics of the devices. As shown in Fig. 2(g), electron-only devices are mounted, and trap-filled limit voltages (V_{TFL}) of 0.28 and 0.16 V are obtained for devices based on pristine SnO_2 and capsaicin-SnO_2, respectively. Usually, the trap density (N_t) is affected by V_{TFL}, as described by the following equation:[39]

$$N_t = \frac{2\varepsilon_0 \varepsilon_r V_{TFL}}{qL^2}, \quad (1)$$

where ε_0, ε_r, q, and L are the vacuum dielectric constant, dielectric constant, elementary charge, and PVSK film thickness, respectively.

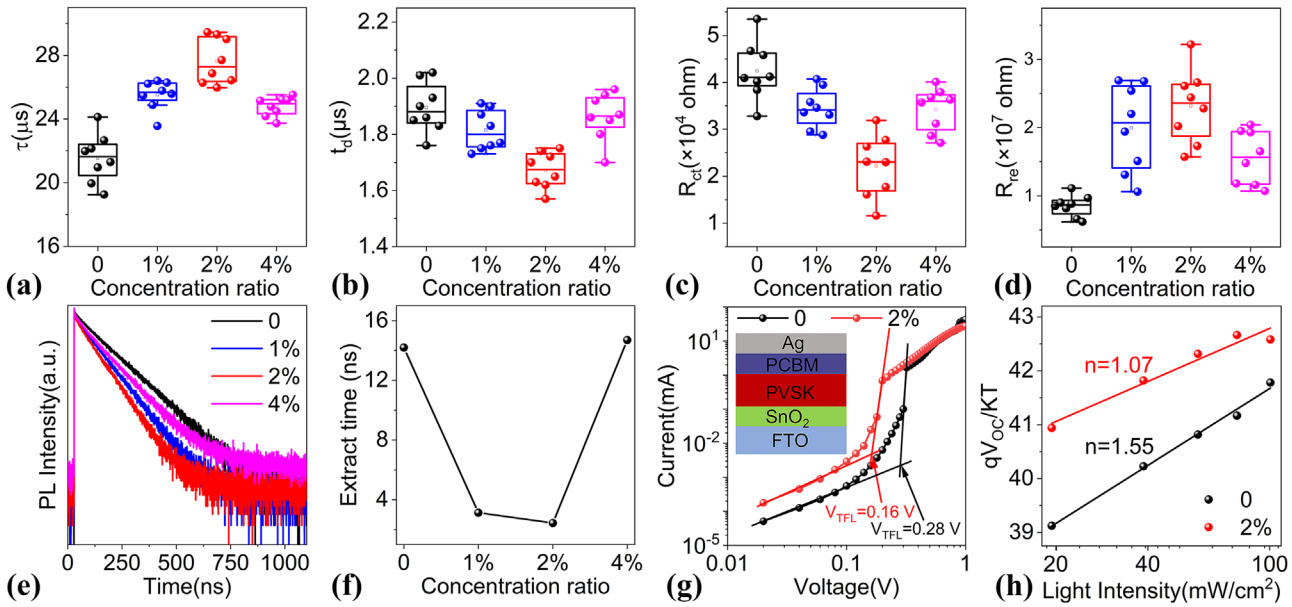

FIG. 2. Effects of capsaicin doping on (a) lifetime (τ), (b) transition time of photogenerated charge carriers (t_d), (c) charge transfer resistance (R_{ct}), (d) recombination resistance (R_{re}), t_d and τ are picked from TPC/TPV curves, respectively, and R_{ct} and R_{re} are picked from the Nyquist plots. (e) The TRPL spectra of the PVSK films deposited on capsaicin-modified SnO_2 substrates, and (f) the extract time picked from TRPL. (g) Dark current–voltage curves of electron-only devices with a structure of "FTO/SnO_2/PVSK/PCBM/Ag" (h) Plotting between qV_{OC}/K_BT and light intensity (presented in logarithm, or ln P).

Accordingly, trap densities of 2.24×10^{15} and 1.28×10^{15} cm^{-3} could be estimated for control and modified device (doping ratio of 2%), respectively. Obviously, capsaicin modification has lowered down the trap density. To further elucidate the charge recombination kinetics, V_{oc} was recorded while changing light intensity. Since photocurrent density of devices scales linearly with the light intensity, with slope near 1 (Fig. S3), thus qV_{OC}/K_BT could be plotted against light intensity according to the following formula:[40]

$$\frac{qV_{OC}}{K_BT} \propto n \ln P, \tag{2}$$

where n, K_B, and T are ideal factor, Boltzmann constant, and the absolute temperature, respectively. Accordingly, the ideal factor of n could be picked by linearly fitting. As seen in Fig. 2(h), for the control device, the slope is 1.55, while for the 2% device, the slope decreases to 1.07, which is closer to 1. Again, this indicates that defect-assisted recombination is suppressed. Moreover, the Mott−Schottky study is performed, and capacitance–voltage (C^{-2}–V) curves are obtained, by which the built-in potential (V_{bi}) is fitted. As show in Fig. S4, 2% device shows higher V_{bi} of 0.92 V, compared to 0.86 V of the control device. The elevated V_{bi} is also ascribed to the lowered trap density. As a result, recombination could be reduced. Meanwhile, the faster charge-extraction process could be anticipated due to the reduced trapping effect.[41]

From above studies, one can find two merits of the capsaicin modification. One is accelerated charge transfer, and the other is the retarded charge recombination. Both of the two are relating to the passivation of the interfacial defects between PVSK and SnO_2. X-ray photoelectron spectroscopy (XPS) study [Fig. 3(a)] observes that, after capsaicin modification, binding energy of $Sn3d_{3/2}$ shifts from 494.8 to 495.5 eV, while that of $Sn3d_{5/2}$ shifts from 486.4 to 487.0 eV. These peaks are mainly due to Sn(IV) according to the experimental details and also the comparison to literatures.[42,43] Moreover, binding energy of O1s also shifts to the higher side [as shown in Fig. 3(b)], and the binding energy at higher and lower sides corresponds to oxygen from hydroxyl group and SnO_2, respectively.[22] Similar behavior was observed in previous reports, whereas SnO_2 was doped with amino trimethylene phosphonic acid or C_{60} pyrrolidine trisacid.[44–46] These positive shifts imply possible charge transfer between capsaicin, which modifies the Fermi level of the SnO_2 matrix and, hence, the larger binding energy.[47,48] Such transfer may happen due to the coordination between carbonyl group (–C=O) from capsaicin and Sn atom, as shown in Fig. 3(d). The possible interaction between capsaicin and PVSK was also studied by XPS.[49] As shown in Fig. 3(c), after capsaicin modification, binding energy of Pb core level also moves to higher side, which shows possible coordination between capsaicin and Pb.[29] In addition, DMF rush brings less effect on the spectrum, thus capsaicin molecules could remain in SnO_2 matrix during the deposition of PbI_2. Such behavior is important for interaction between capsaicin and both SnO_2 and PVSK. Moreover, no significant shift is seen for the N1s peak (Fig. S5), showing that interaction between the amine group (-NH) and SnO_2 might be weaker.

Moreover, charge density of SnO_2/capsaicin interface and PVSK/capsaicin interfaces is calculated using the vienna *ab initio* simulation package (VASP) code (details are shown in the supplementary material). The results are shown in Figs. 3(c) and 3(d). It can be seen that the charge exchange mainly occurs between O-Sn and O-Pb. In addition, "bader charges" analysis is performed, which is usually used to calculate the charge number accumulating around a particular atom.[50] In the current study, the bader charges of the two Sn atoms

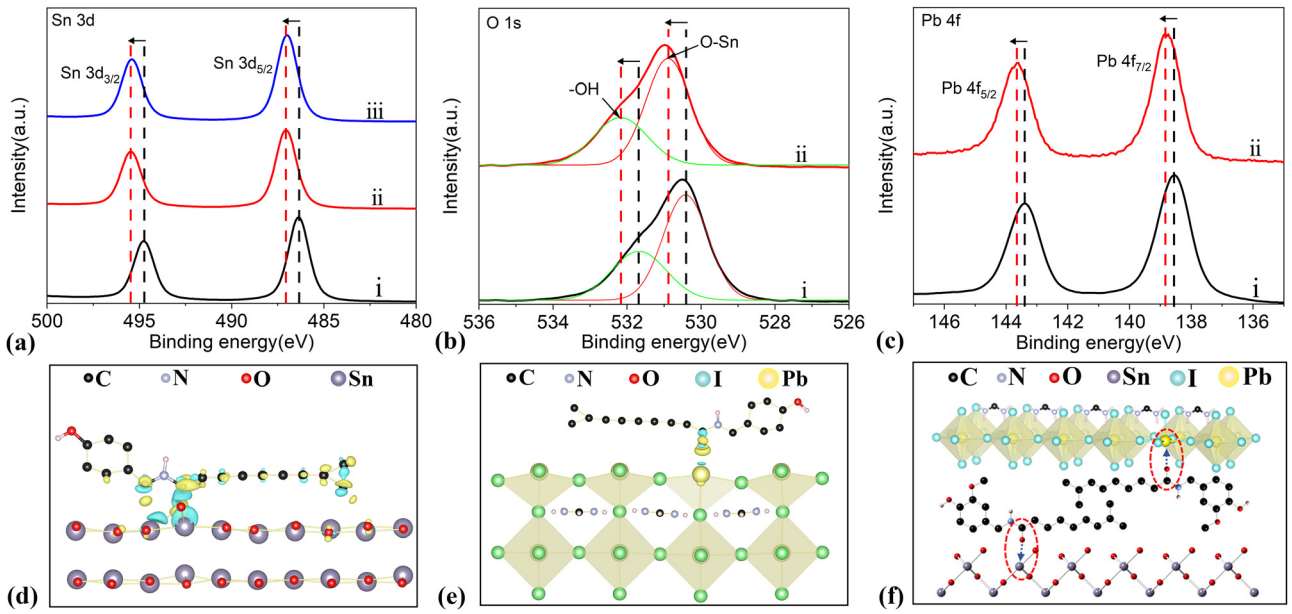

FIG. 3. X-ray photoelectron spectroscopy showing the binding energy of (a) Sn and (b) O of SnO_2, and (c) Pb from PVSK that grown on SnO_2; i, ii, and iii correspond to SnO_2, SnO_2 @ Capsaicin, and SnO_2 @ Capsaicin with DMF rush, respectively. Charge density of (d) SnO_2/capsaicin and (e) capsaicin/PVSK interface. The green and yellow areas represent the electron accumulation and depletion, respectively. (f) Schematic for the interaction between capsaicin and both SnO_2 and PVSK, and the interaction is marked by the blue arrow in circles.

adjacent to O atom (from carbonyl group of capsaicin) are 2.81 and 3.14, both are lower than 4, while that of the O atoms (from the carbonyl) is 7.17. Similarly, bader charge of Pb atom adjacent to the O atom is 3.07 (<4), while that of the corresponding O atom is 7.08. As such, obvious interaction takes place between capsaicin molecule and both SnO_2 and PVSK, as shown in Fig. 3(f).

Photostability and storage stability are evaluated. As shown in Fig. S6, better stability is harvested after capsaicin doping. Typically, after 1000-h storage, the modified device maintains about 90% of the original PCE, compared to 76% of the control devices. As such, capsaicin modification improved device stability. This arises for two reasons: (i) The hydrophobicity of the capsaicin molecule prevents the penetration of water vapor; (ii) The capsaicin-SnO_2 substrate promotes crystal quality of PVSK. The first aspect could be reflected from contact angle test. From Figs. S7(a)–S7(d), one can see that capsaicin doping increases the hydrophobicity of the SnO_2 film, which is due to the long carbon chain of the molecule. The second aspect could be reflected from combined examination on SnO_2 ETM surface and PVSK crystallinity. Atomic force microscope (AFM) study shows that the capsaicin doping flattens SnO_2 surface [shown in Figs. S7(e)–S7(h)]. Meanwhile, relatively larger grains and smaller PbI_2/PVSK ratio could be seen in the PVSK film when it is coated on capsaicin doped SnO_2 ETM (as shown in Figs. S8 and S9). In fact, similar phenomenon was observed by Bi *et al.*[51] It is suggested that the increased hydrophobicity on substrate could suppress the heterogeneous nucleation, and hence favor the crystal growth. The improved crystallinity could also contribute to better device stability.[52]

In summary, with capsaicin modification, defect density of the PSCs is reduced, which is due to the interaction between capsaicin and SnO_2 and PVSK, concretely between–C═O group and both Sn and Pb atoms (or ions). The passivation accelerates charge transfer and reduces recombination. In addition, the passivation is realized by directly adding capsaicin into SnO_2 QDs matrix; this strategy could reduce the complexity of passivation.

See the supplementary material for the device preparation and characterization and the schematic of the device structure (Fig. S1); typical TPV/TPC and Nyquist plots (Fig. S2); plotting between J_{sc} and light intensity (Fig. S3); Mott−Schottky study of devices (Fig. S4); XPS of N1s (Fig. S5); photostability and storage-stability (Fig. S6); wettability test of capsaicin-doped SnO_2 and AFM images of capsaicin-doped SnO_2 (Fig. S7); top view and cross section of SEM images of PVSK coated on capsaicin-doped SnO_2 (Fig. S8); XRD pattern of PVSK films (Fig. S9); fitted results of TRPL curves (Table S1).

C. Zhou thanks the financial support of the National Natural Science Foundation of China (NSFC, No. 61774170) and the Natural Science Foundation of Hunan Province (No. 2020JJ4759). S. Lin acknowledges the financial support from the Fundamental Research Funds for the Central South University (No. 2020zzts045). Y. Gao acknowledges the support from the National Science Foundation, United States (NSF No. DMR-1903962). Y. Hu and W. Zhang thank the financial support from the National Natural Science Foundation of China (NSFC, No. 22075094). We acknowledge the helpful discussion with Professor Haipeng Xie from CSU regarding to the XPS analysis.

AUTHOR DECLARATIONS

Conflict of Interest

The authors declare no conflict of interest.

DATA AVAILABILITY

The data that support the findings of this study are available within the article and its supplementary material.

REFERENCES

[1]A. Kojima, K. Teshima, Y. Shirai, and T. Miyasaka, J. Am. Chem. Soc. **131**(17), 6050 (2009).
[2]Q. Jiang, Y. Zhao, X. Zhang, X. Yang, Y. Chen, Z. Chu, Q. Ye, X. Li, Z. Yin, and J. You, Nat. Photonics **13**(7), 460 (2019).
[3]C. Ma and N.-G. Park, Chem **6**(6), 1254 (2020).
[4]J. J. Yoo, G. Seo, M. R. Chua, T. G. Park, Y. Lu, F. Rotermund, Y.-K. Kim, C. S. Moon, N. J. Jeon, J.-P. Correa-Baena, V. Bulović, S. S. Shin, M. G. Bawendi, and J. Seo, Nature **590**(7847), 587 (2021).
[5]H. Min, D. Y. Lee, J. Kim, G. Kim, K. S. Lee, J. Kim, M. J. Paik, Y. K. Kim, K. S. Kim, M. G. Kim, T. J. Shin, and S. I. Seok, Nature **598**(7881), 444 (2021).
[6]W. Shockley and H. J. Queisser, J. Appl. Phys. **32**(3), 510 (1961).
[7]I. M. Peters and T. Buonassisi, Joule **2**(6), 1160 (2018).
[8]N. Marinova, W. Tress, R. Humphry-Baker, M. I. Dar, V. Bojinov, S. M. Zakeeruddin, M. K. Nazeeruddin, and M. Gratzel, ACS Nano **9**(4), 4200 (2015).
[9]E. Guillén, F. J. Ramos, J. A. Anta, and S. Ahmad, J. Phys. Chem. C **118**(40), 22913 (2014).
[10]S. P. Pang, H. Hu, J. L. Zhang, S. L. Lv, Y. M. Yu, F. Wei, T. S. Qin, H. X. Xu, Z. H. Liu, and G. L. Cui, Chem. Mater. **26**(3), 1485 (2014).
[11]Y. Wang, Y. Yue, X. Yang, and L. Han, Adv. Energy Mater. **8**(22), 1800249 (2018).
[12]K. Xiao, R. Lin, Q. Han, Y. Hou, Z. Qin, H. T. Nguyen, J. Wen, M. Wei, V. Yeddu, M. I. Saidaminov, Y. Gao, X. Luo, Y. Wang, H. Gao, C. Zhang, J. Xu, J. Zhu, E. H. Sargent, and H. Tan, Nat. Energy **5**(11), 870 (2020).
[13]J. J. Xue, R. Wang, and Y. Yang, Nat. Rev. Mater. **5**(11), 809 (2020).
[14]N. J. Jeon, H. Na, E. H. Jung, T.-Y. Yang, Y. G. Lee, G. Kim, H.-W. Shin, S. I. Seok, J. Lee, and J. Seo, Nat. Energy **3**(8), 682 (2018).
[15]J. Jeong, M. Kim, J. Seo, H. Lu, P. Ahlawat, A. Mishra, Y. Yang, M. A. Hope, F. T. Eickemeyer, M. Kim, Y. J. Yoon, I. W. Choi, B. P. Darwich, S. J. Choi, Y. Jo, J. H. Lee, B. Walker, S. M. Zakeeruddin, L. Emsley, U. Rothlisberger, A. Hagfeldt, D. S. Kim, M. Gratzel, and J. Y. Kim, Nature **592**(7854), 381 (2021).
[16]T. Ye, J. Xing, M. Petrović, S. Chen, V. Chellappan, G. Sandhya Subramanian, T. Chien Sum, B. Liu, Q. Xiong, and S. Ramakrishna, Sol. Energy Mater. Sol. Cells **163**, 242 (2017).
[17]G. Liu, B. Yang, B. Liu, C. Zhang, S. Xiao, Y. Yuan, H. Xie, D. Niu, J. Yang, Y. Gao, and C. Zhou, Appl. Phys. Lett. **111**(15), 153501 (2017).
[18]P. F. Méndez, S. K. M. Muhammed, E. M. Barea, S. Masi, and I. Mora-Seró, Sol. RRL **3**(9), 1900191 (2019).
[19]Q. Jiang, X. Zhang, and J. You, Small **14**(31), e1801154 (2018).
[20]Q. Jiang, L. Zhang, H. Wang, X. Yang, J. Meng, H. Liu, Z. Yin, J. Wu, X. Zhang, and J. You, Nat. Energy **2**(1), 16177 (2016).
[21]W. Ke, G. Fang, Q. Liu, L. Xiong, P. Qin, H. Tao, J. Wang, H. Lei, B. Li, J. Wan, G. Yang, and Y. Yan, J. Am. Chem. Soc. **137**(21), 6730 (2015).
[22]G. Yang, C. Chen, F. Yao, Z. Chen, Q. Zhang, X. Zheng, J. Ma, H. Lei, P. Qin, L. Xiong, W. Ke, G. Li, Y. Yan, and G. Fang, Adv. Mater. **30**(14), e1706023 (2018).
[23]S. Mahesh, J. M. Ball, R. D. J. Oliver, D. P. McMeekin, P. K. Nayak, M. B. Johnston, and H. J. Snaith, Energy Environ. Sci. **13**(1), 258 (2020).
[24]P. Chen, Y. Bai, and L. Wang, Small Struct. **2**(1), 2000050 (2021).
[25]W. Ke, D. Zhao, C. Xiao, C. Wang, A. J. Cimaroli, C. R. Grice, M. Yang, Z. Li, C.-S. Jiang, M. Al-Jassim, K. Zhu, M. G. Kanatzidis, G. Fang, and Y. Yan, J. Mater. Chem. A **4**(37), 14276 (2016).
[26]D. Yang, R. Yang, K. Wang, C. Wu, X. Zhu, J. Feng, X. Ren, G. Fang, S. Priya, and S. F. Liu, Nat. Commun. **9**(1), 3239 (2018).

[27]J. Zhuang, P. Mao, Y. Luan, N. Chen, X. Cao, G. Niu, F. Jia, F. Wang, S. Cao, and J. Wang, Adv. Funct. Mater. **31**(17), 2010385 (2021).
[28]P. Y. Wang, B. B. Chen, R. J. Li, S. L. Wang, N. Y. Ren, Y. C. Li, S. Mazumdar, B. A. Shi, Y. Zhao, and X. D. Zhang, ACS Energy Lett. **6**(6), 2121 (2021).
[29]S. Xiong, Z. Hou, S. Zou, X. Lu, J. Yang, T. Hao, Z. Zhou, J. Xu, Y. Zeng, W. Xiao, W. Dong, D. Li, X. Wang, Z. Hu, L. Sun, Y. Wu, X. Liu, L. Ding, Z. Sun, M. Fahlman, and Q. Bao, Joule **5**(2), 467 (2021).
[30]W.-Q. Wu, J.-X. Zhong, J.-F. Liao, C. Zhang, Y. Zhou, W. Feng, L. Ding, L. Wang, and D.-B. Kuang, Nano Energy **75**, 104929 (2020).
[31]Z.-S. Wang, H. Kawauchi, T. Kashima, and H. Arakawa, Coordin. Chem. Rev. **248**(13–14), 1381 (2004).
[32]F. Gao, Y. Wang, D. Shi, J. Zhang, M. Wang, X. Jing, R. Humphry-Baker, P. Wang, S. M. Zakeeruddin, and M. Gratzel, J. Am. Chem. Soc. **130**(32), 10720 (2008).
[33]P. Xia, D. Guo, S. Lin, S. Liu, H. Huang, D. Kong, Y. Gao, W. Zhang, Y. Hu, and C. Zhou, Sol. RRL **5**(11), 2100408 (2021).
[34]H. Chen, K. Li, H. Liu, Y. Gao, Y. Yuan, B. Yang, and C. Zhou, Org. Electron. **61**, 119 (2018).
[35]T. Shi, S. Lin, M. Fang, D. Kong, Y. Yuan, Y. Gao, B. Yang, H. Han, and C. Zhou, Appl. Phys. Lett. **117**(16), 163501 (2020).
[36]G. Liu, B. Yang, H. Chen, Y. Zhao, H. Xie, Y. Yuan, Y. Gao, and C. Zhou, Appl. Phys. Lett. **115**(21), 213501 (2019).
[37]Q.-Q. Chu, B. Ding, J. Peng, H. Shen, X. Li, Y. Liu, C.-X. Li, C.-J. Li, G.-J. Yang, T. P. White, and K. R. Catchpole, J. Mater. Sci. Technol. **35**(6), 987 (2019).
[38]Y. Chen, X. Zuo, Y. He, F. Qian, S. Zuo, Y. Zhang, L. Liang, Z. Chen, K. Zhao, Z. Liu, J. Gou, and S. Liu, Adv. Sci. **8**(5), 2001466 (2021).
[39]P. N. Murgatroyd, J. Phys. D **3**(2), 151 (1970).
[40]Y. Li, J. Shi, B. Yu, B. Duan, J. Wu, H. Li, D. Li, Y. Luo, H. Wu, and Q. Meng, Joule **4**(2), 472 (2020).
[41]Y. Shao, Z. Xiao, C. Bi, Y. Yuan, and J. Huang, Nat. Commun. **5**, 5784 (2014).
[42]I.-T. Cho, U. Myeonghun, S.-H. Song, J.-H. Lee, and H.-I. Kwon, Semicond. Sci. Technol. **29**(4), 045001 (2014).
[43]K. Nose, A. Y. Suzuki, N. Oda, M. Kamiko, and Y. Mitsuda, Appl. Phys. Lett. **104**(9), 091905 (2014).
[44]J. Zhang, R. Li, S. Apergi, P. Wang, B. Shi, J. Jiang, N. Ren, W. Han, Q. Huang, G. Brocks, Y. Zhao, S. Tao, and X. Zhang, Sol. RRL **5**(10), 2100464 (2021).
[45]B. Tu, Y. Shao, W. Chen, Y. Wu, X. Li, Y. He, J. Li, F. Liu, Z. Zhang, Y. Lin, X. Lan, L. Xu, X. Shi, A. M. C. Ng, H. Li, L. W. Chung, A. B. Djurisic, and Z. He, Adv. Mater. **31**(15), e1805944 (2019).
[46]S.-K. Huang, Y.-C. Wang, W.-C. Ke, Y.-T. Kao, N.-Z. She, J.-X. Li, C.-W. Luo, A. Yabushita, D.-Y. Wang, Y. J. Chang, K. Tsukagoshi, and C.-W. Chen, J. Mater. Chem. A **8**(44), 23607 (2020).
[47]Y. Gao, Mater. Sci. Eng., R **68**(3), 39 (2010).
[48]L. Li, X. Liu, L. Lyu, R. Wu, P. Liu, Y. Zhang, Y. Zhao, H. Wang, D. Niu, J. Yang, and Y. Gao, J. Phys. Chem. C **120**(32), 17863 (2016).
[49]Z. Dai, S. K. Yadavalli, M. Chen, A. Abbaspourtamijani, Y. Qi, and N. P. Padture, Science **372**(6542), 618 (2021).
[50]B. Liu, M. Long, M. Cai, L. Ding, and J. Yang, Nano Energy **59**, 715 (2019).
[51]C. Bi, Q. Wang, Y. Shao, Y. Yuan, Z. Xiao, and J. Huang, Nat. Commun. **6**, 7747 (2015).
[52]S. Liu, D. Zhang, Y. Sheng, W. Zhang, Z. Qin, M. Qin, S. Li, Y. Wang, C. Gao, Q. Wang, Y. Ming, C. Liu, K. Yang, Q. Huang, J. Qi, Q. Gao, K. Chen, Y. Hu, Y. Rong, X. Lu, A. Mei, and H. Han, "Highly oriented MAPbI3 crystals for efficient hole-conductor-free printable mesoscopic perovskite solar cells," Fundam. Res. (to be published).